Int J Clin Exp Med 2017;10(4):6429-6436
www.ijcem.com /ISSN:1940-5901/IJCEM0042986

Original Article

Establishment of a rabbit model of pectus excavatum

Ruchen Wang[1*], Weilin Yang[2*], Lie Cai[3], Jianyong Yang[4], Xianhong Xiang[4], Chaohui Zhang[4], Qing Jiang[5], Yuexiong Yang[6], Zhenguang Chen[1,2,7*]

Departments of [1]Thoracic Surgery, [2]Cardiothoracic Surgery of East Division, [3]Central Sterile Supply, [4]Interventional Radiology, The First Affiliated Hospital, Sun Yat-sen University, Guangzhou, China; [5]School of Engineering, Sun Yat-sen University, Guangzhou, China; [6]Guangzhou Zhongda Medical Apparatus and Instruments Company, Guangzhou, China; [7]Lung Cancer Research Center of Sun Yat-sen University, Guangzhou, China. [*]Equal contributors.

Received October 27, 2016; Accepted December 30, 2016; Epub April 15, 2017; Published April 30, 2017

Abstract: Background: Pectus excavatum (PE) is the most common chest wall malformation. The main treatments of PE are the Nuss and Ravitch procedures. Because the pathogenesis of PE remains unclear, an exact animal model has been difficult to establish. Animal models are unavailable to test new steel bars used in the Nuss procedure and to elucidate the mechanism by which PE affects pulmonary function. This study described the establishment of a rabbit model of PE. Methods: Twenty-four New Zealand white rabbits were randomized into a PE group and a control group. The animals in the PE group underwent surgery to remove a 0.5 cm long segment of the fifth to seventh costicartilage and removal of the sternum at the fifth costicartilage level. In control animals, the skin and muscle were incised and stitched into two layers. Results: Ten days after surgery, rabbits in the PE group showed gradual depression of the sternum. Over time, as rabbit weight increased, the depression of the anterior and inferior chest wall deepened and widened gradually. The deformity of the chest wall was similar at 6 and 12 weeks after surgery. Chest CT scans at 8 weeks after surgery showed that the depression extended from the cutting at the fifth costicartilage level to the spine. Three-dimensional reconstruction of the thorax showed that the depression of the sternum began at the level of fifth rib and most obvious at the level of the seventh rib. Conclusions: This rabbit model of PE was simple, less invasive, and easy to establish.

Keywords: Pectus excavatum, fracture of rib ring, rabbit

Introduction

Pectus excavatum (PE), the most common type of chest wall malformation, with an incidence of 23 per 10,000 live births, is characterized by depression of the anterior and inferior chest wall [1]. PE is 5 times more frequent in men than in women [2], has a strong familial tendency and tends to be polygenetic, with patients showing autosomal dominant, autosomal recessive, and X-linked inheritance [3-5]. Deformations occurring in patients with PE may be symmetric or asymmetric. These anomalies are thought to be caused by the unbalanced growth of the costicartilage region of the anterior and inferior chest wall; if the speed of growth of the costicartilage is faster than that of the sternum, the sternum will be pressed downward, resulting in deformation [6]. PE may have deleterious effects on patients' physical and mental health.

Although PE is often regarded as a cosmetic condition, it has been reported to affect pulmonary function [7]. Patients with mild PE may be asymptomatic, whereas patients with severe PE may experience compression of the heart and lungs. Dyspnea during exercise and chest pains are the most common symptoms in patients with PE [8]. Embarrassment about the deformation may lead to mental illness and reduced quality of life [9-11]. Moreover, PE has been reported to reduce life expectancy [12].

Abnormal pulmonary function in some patients with PE may be due to lung distortion resulting from compression by the depressed anterior and inferior chest wall and the ribs. However, the specific mechanism by which PE affects pulmonary function remains unknown. Animal models of PE may help determine this mechanism. The Haller index on CT scans is important in determining whether or not to surgically treat

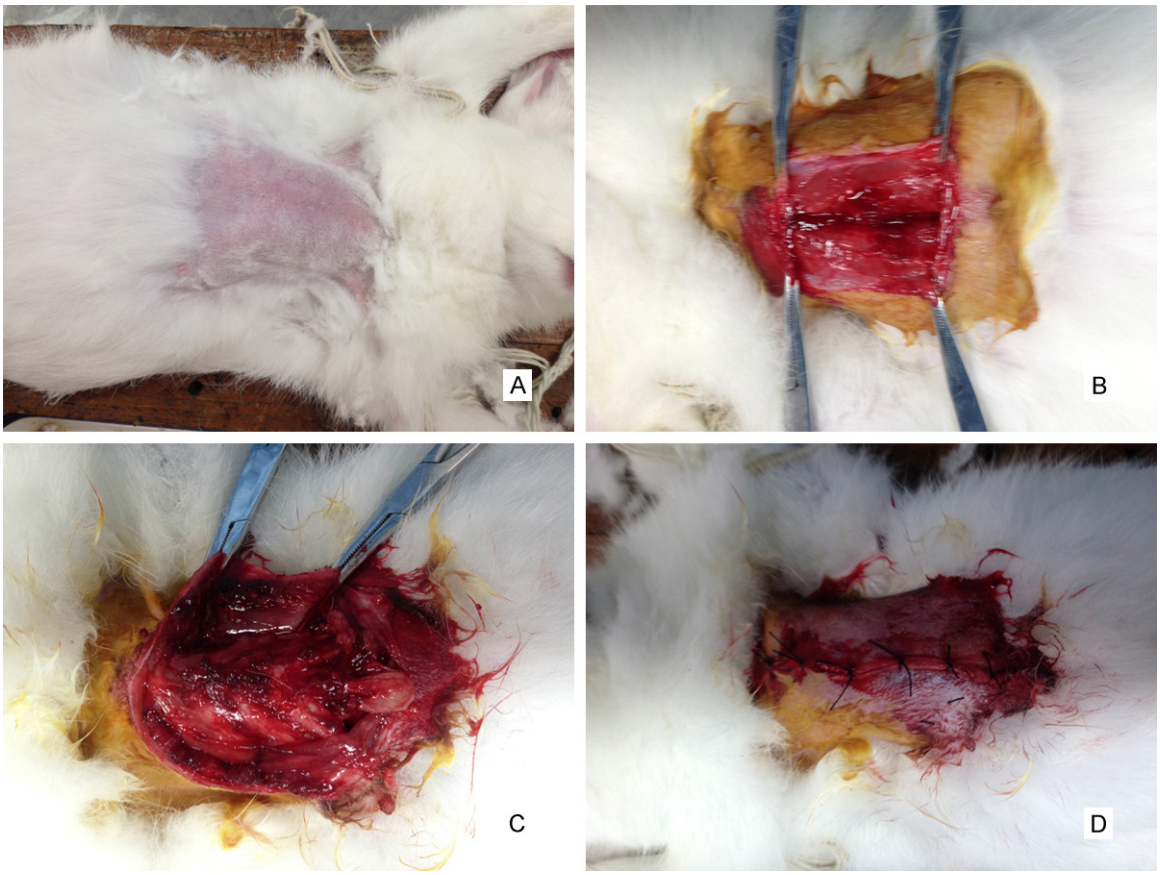

Figure 1. Diagram of Experimental protocol. A. Rabbits were fixed on the operating table on dorsal position after the performance of anaesthesia and removing the hair. B. Skin and muscle before sternum was incised. C. The fifth to seventh costicartilage was exposed when skin and muscle before sternum was incised. D. Incision was stitched in two layers after the operation.

patients with PE, with surgery considered necessary when the Haller index is above 3.125. The main types of surgery for PE are the Nuss and Ravitch procedures. Surgery is not necessary for patients with slight deformation of the chest wall. The Nuss procedure is minimally invasive and simple to perform, and the effects of correction remain good [13]. In the Nuss procedure, which is being increasingly performed worldwide, a steel plate is used to elevate the sternum. As technology advances, new steel plates are introduced to replace the traditional steel plates [14]. Before their use clinically, new steel plates must be tested in animal models to determine their biocompatibility and mechanical characteristics. Proper animal models to test new steel bars and to elucidate the mechanism by which PE affects pulmonary function are lacking. This study describes the development of a rabbit model of PE.

Materials and methods

Laboratory animals

This research was approved by the Animal Research Committee at the Animal Experimental Center of Sun Yat-sen University (Permission Code: SCXK200-8-0002) and conformed to the National Institute of Health Guidelines for the Care and Use of Laboratory Animals. Twenty-four male and female, specific-pathogen-free New Zealand white rabbits, weighing 1.8-2.2 kg and bred at the Animal Center of Sun Yat-sen University, were maintained in individual cages in a temperature-regulated (24°C) room at the animal center and allowed free access to rabbit chow and water.

Major instruments and apparatus

CT was performed using a 64-multidetector spiral CT (Aquilion ViSION, Toshiba Company of

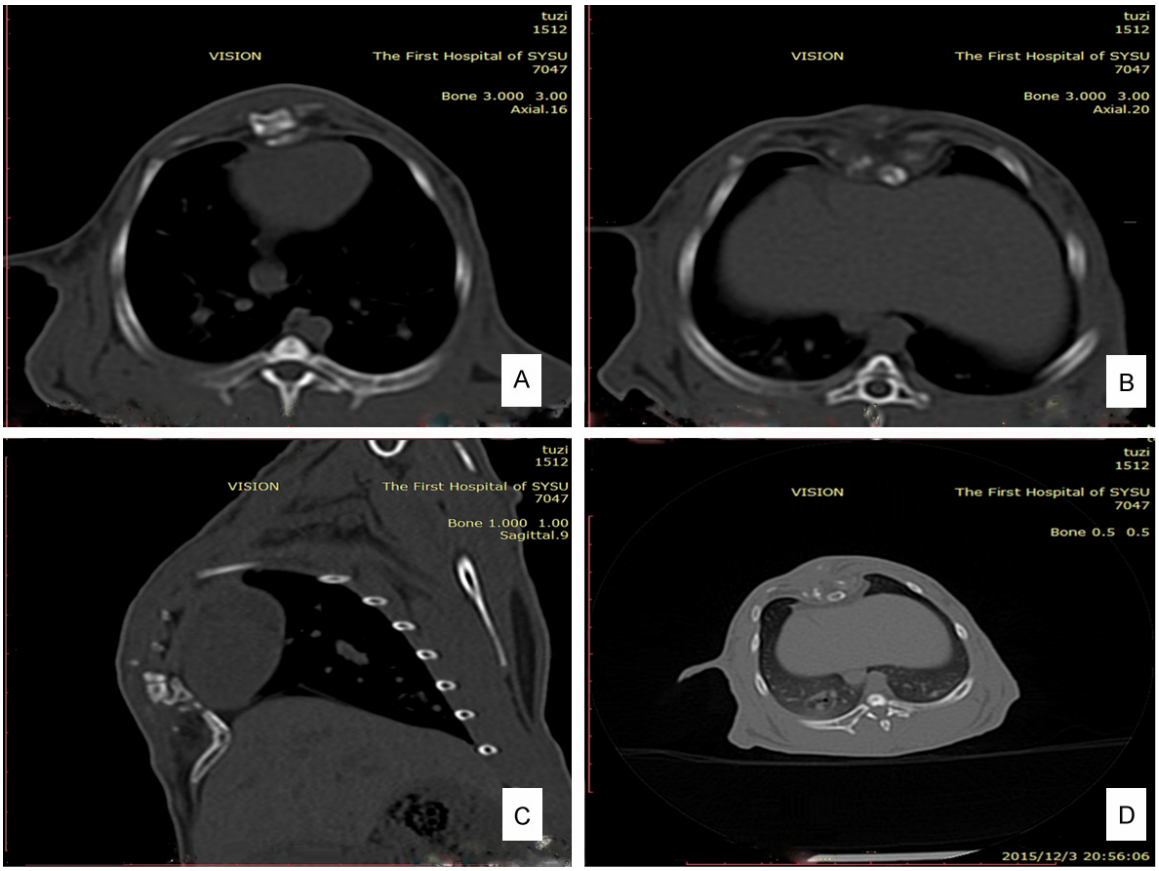

Figure 2. Chest CT appearance of rabbit models of PE. A. The depression was from the cutting at fifth costicartilage level and was asymmetrical. B. The depression was most obvious in this image and the sternum was inclined to the left. C. Coronal reconstructed image. D. The depression was obvious in this image and the sternum was inclined to the left.

Japan). General surgical instruments were obtained from the Animal Experimental Center of Sun Yat-sen University and surgical sutures (from Johnson & Johnson, USA).

Experimental protocol

The 24 animals were randomly divided into two groups (n=12 for each) and anesthetized by injection into the auricular veins of 3% pentobarbital (1 mL/kg). Hair on the anterior chest wall was removed with an electric shaver, and the area was disinfected with povidone-iodine. Rabbits were fixed on the operating table in the dorsal position. A 7 cm long median longitudinal incision was made in the xiphoid process. The skin and muscle in front of the sternum was incised, exposing the structural connection of the ribs and cartilage. The seventh costal connected to the sternum was identified as the lowermost costicartilage. Rabbits in the PE group underwent removal of a 0.5 cm long segment of the fifth to seventh costicartilage, taking care to protect the pleura so as not to induce pneumothorax. The sternum was subsequently removed at the level of the fifth costicartilage (**Figure 1**). In control animals, the skin and muscle were incised and stitched into two layers. All rabbits received postoperative intramuscular injections of antibiotics for 3 days to prevent infection.

Main outcome measures

Rabbits were followed-up for 12 weeks after the operation, during which time changes in chest wall appearance were monitored. All rabbits underwent chest CT scans 8 weeks after surgery, to obtain sagittal, coronal and cross-sectional images of the rabbits' chest walls, followed by 3-dimensional reconstruction using DICOM data and Mimmics 16 software. The length, width and depth of the depression in each rabbit were determined from the 3D images using Magics 9.5.

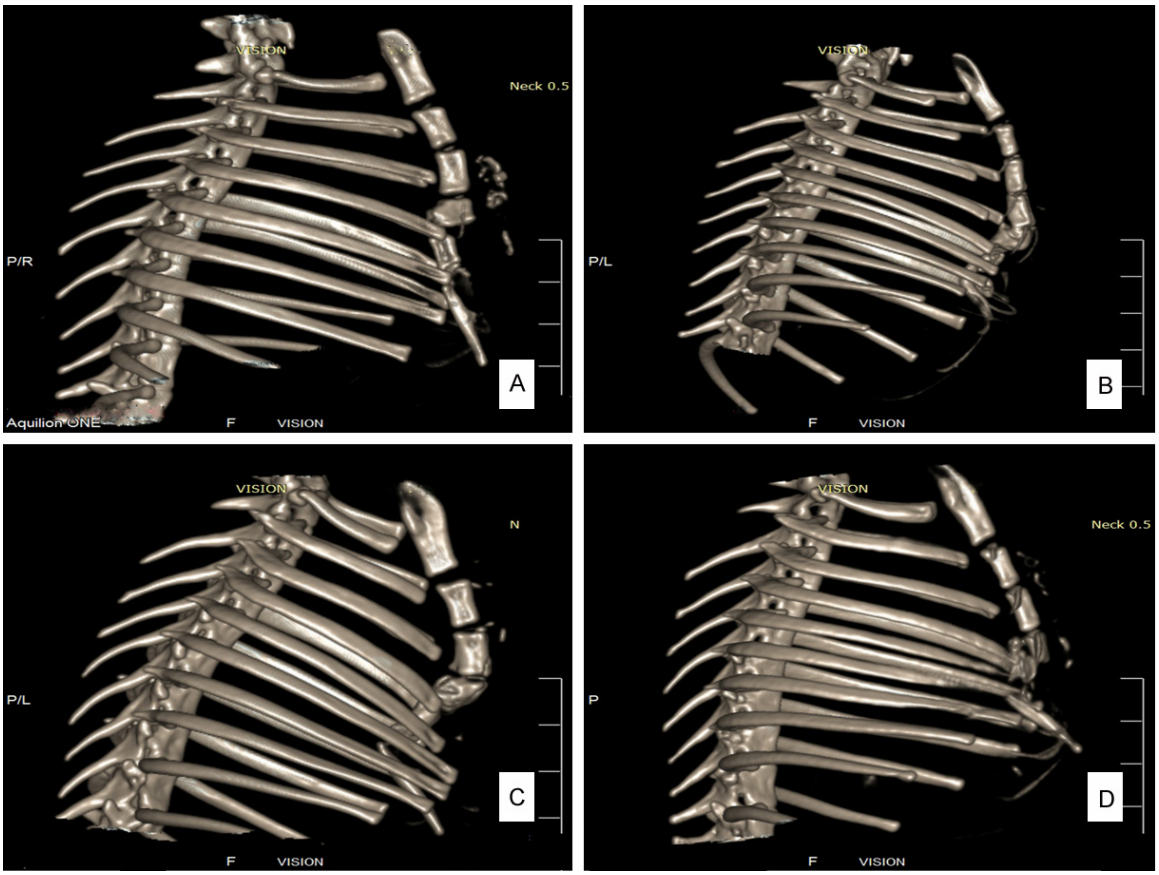

Figure 3. Dimensions of depressions in the rabbit PE model. A. The three-dimensional reconstruction of thorax of experimental group. B. The three-dimensional reconstruction of thorax of experimental group showed that the depression of sternum was from the level of fifth rib and the depression was most obvious at the level of seventh rib. It can be seen from the three-dimensional reconstruction that the depression shifted upwards from the deepest sag at the level of seventh rib. The malformation was like a boat in the profile of three-dimensional reconstruction of thorax of rabbit. C. The three-dimensional reconstruction of thorax of experimental group. D. The three-dimensional reconstruction of thorax of experimental group.

Results

Changes in chest wall appearance

Paradoxical respiration was observed after surgery in both the control and experimental groups, but vanished after anesthesia wore off. Pectus carinatum-like changes due to swelling in local tissues were observed in the anterior and inferior chest wall 1-5 days after surgery. Gradually depression in the region of the sternum was observed in the experimental group 10 days after the operation, deepening at 2 weeks. At 3 weeks, this depression, located at the junction of the sternum and xiphoid center, widened and formed a malformation typical of PE. Over time, as rabbit weight increased, the depression of the anterior and inferior chest wall deepened and widened. Beginning 5 weeks after surgery, malformation of rabbit chest wall was not proportional to the increase in weight. The deformity of the chest wall at 12 weeks was similar to that at 6 weeks.

Chest CT appearance

Chest CT scans of the PE group showed that the depression extended from the cutting at the fifth costicartilage level to the spine. Chest CT also showed that the sternum was cut and corresponding ribs amputated. Three-dimensional reconstruction of the thorax of rabbits in the PE group showed that the depression of the sternum extended from the level of fifth rib and was most obvious at the level of seventh rib. The three-dimensional reconstruction showed that the depression shifted upwards from the deepest sag at the level of seventh rib

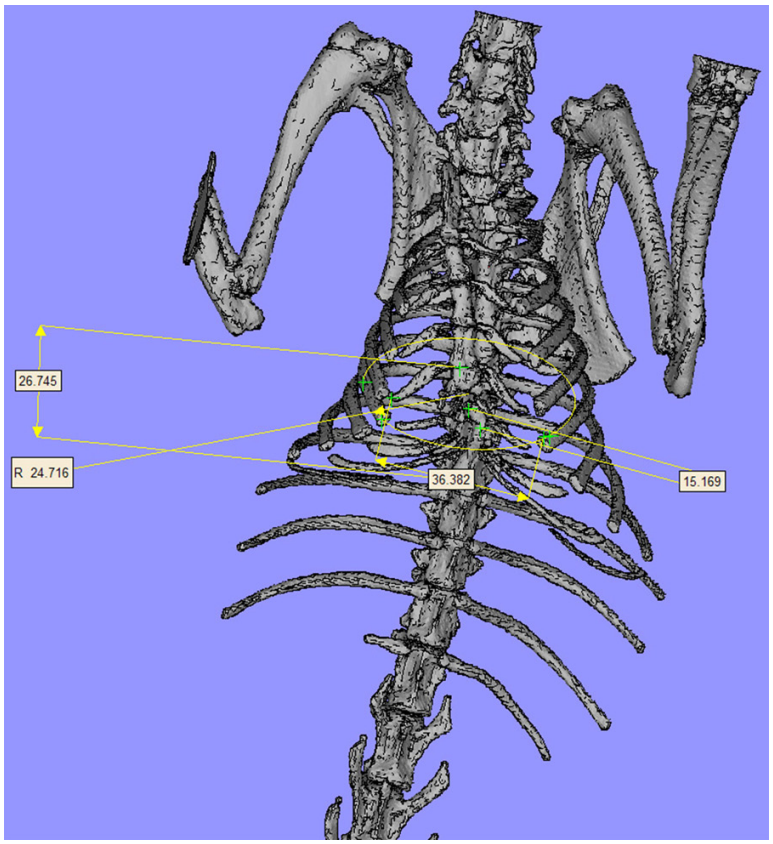

Figure 4. Measurement drawing of 3D image of one rabbit.

Table 1. Length, width and depth of the depression in rabbits

	Low (mm)	High (mm)	Average (mm)	Standard Deviation
Length	23.688	39.964	29.015	5.98
Width	28.518	36.282	33	3.41
Depth	9.57	15.169	12.45	4.04

and that the malformation had a boat-like appearance (**Figure 2**). The deformity was symmetrical when viewed by chest CT from the outside, but was asymmetric when viewed from the inside.

Dimensions of depressions in the rabbit PE model

Measurement drawings of 3D images were obtained using Magics 9.5 software package (**Figures 3**, **4**). This software was also used to characterize the length, width and depth of anterior and inferior depressions in these rabbits (**Table 1**).

Discussion

To date, the pathogenesis of PE has remained unclear, especially since exact animal models are difficult to establish. The modified Ravitch procedure consists of three steps: 1) exposure of the sternum and surrounding area; 2) removal of abnormal cartilage; and 3) fixing the sternum in a more normal position using a metal bar, which remains in place for at least 1 year and is removed surgically later [15]. PE may recur, however, after the Ravitch procedure [16], perhaps because removal of abnormal cartilage and fixation of the sternum may lead to a softened chest wall. Intrathoracic negative pressure is required to maintain spontaneous breathing. Differential pressure between the outside and inside of the chest wall may lead to chest wall depression due its softening. PE recurrence after the Ravitch procedure may be attributed to the softened chest wall and intrathoracic negative pressure. Animal models of PE may be generated by cutting the lowermost parts of the cartilage and the corresponding level of the sternum.

A mouse model of PE and scoliosis was generated by knockout of Gpr126/Adgrg6 [17], with Gpr126 found to be a genetic cause for the pathogenesis of AIS and PE. This model is difficult to replicate, because Gpr126/Adgrg6 knockout mice are very expensive. Moreover, the size of these animals makes it difficult to test the biocompatibility and mechanical characteristics of new steel bars. Changes in the chest walls of patients with PE after Nuss bar removal and deformations caused by bars and stabilizers were assessed by three-dimensional reconstructions of multislice CT scans [18]. These high-resolution, three-dimensional images of the thoracic cavity are considered an ideal imaging model to compare operation associated differences in the chest wall. The imaging

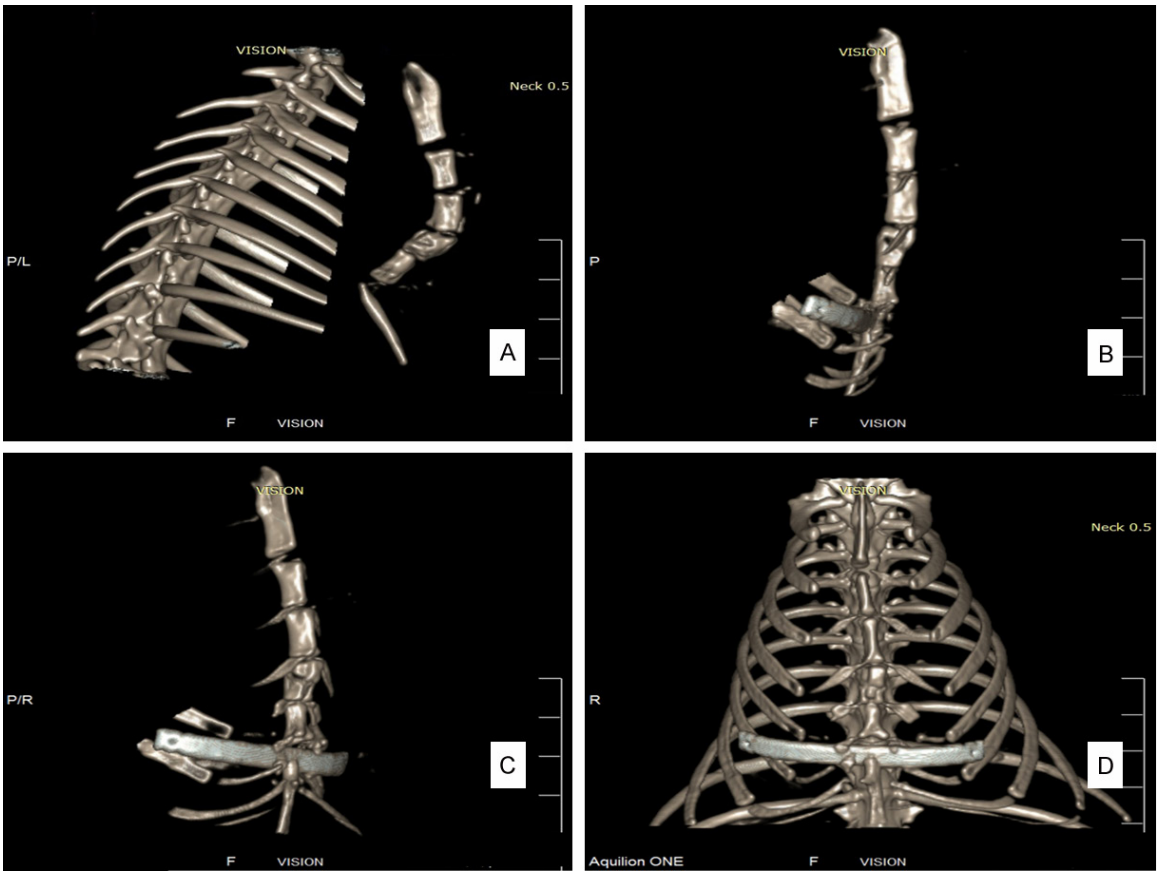

Figure 5. Testing of 3D printed Titanium Alloy implant in the rabbit model of PE. A. 3D reconstruction of Chest CT of rabbit model before operation; B. 3D reconstruction of Chest CT of rabbit model after operation; C. 3D reconstruction of Chest CT of rabbit model after operation; D. 3D reconstruction of Chest CT of rabbit model after operation.

model can provide a theoretical basis for individualized treatment of patients with PE [19-21]. Artificial neural networks were used to automatically model of corrective prostheses in PE, thus eliminating the exposure to radiation associated with CT [22]. This imaging model based on artificial neural networks was comparable with the imaging model based on CT scanning, but the former was unable to assess the mechanical and biological characteristics of PE.

Rabbits are used as models for many diseases, including acute myocardial infarction and scoliosis [23, 24]. Our rabbit model of PE is similar to the human disease on imaging, but differs in mechanism and inducing factors. Nevertheless, this rabbit model can be used to test the mechanical and biological characteristics of new steel bars used in the Nuss procedure and to assess operative changes in lung function. In the absence of an appropriate model, individual animal models must be used to assess the mechanical and biological characteristics of new steel bars, such as the use of pig chest wall to test mechanical characteristics date and the use of guinea pigs to test biological characteristics [25]. The rabbit model of PE can also be used to test the teratogenicity and carcinogenicity of new bars.

Normal breathing depends on the integrity of the chest wall. Use of our rabbit model indicated that fracture of a rib ring can cause PE. Fracture of the rib ring resulting in PE can occur during pediatric surgery and cardiothoracic surgery, making it important to protect the rib ring during these operations.

Compared with PE models based on complex gene knockout technology and complicated image-based software, our rabbit model of PE was easy to establish. It is important, however, to maintain the integrity of the pleura during the operation. Cutting the ribs and the corresponding level of sternum is easy to perform.

Use of this model to assess the etiology of PE and to test new bars used in the Nuss procedure can avoid ethical issues.

In our further experiment, we individually corrected this rabbit model of PE by using the 3D printed Titanium Alloy implant. 3D printed Titanium Alloy implants were made according to mechanical parameters of chest of rabbit and the shape of rabbit model of PE. 3D printed Titanium Alloy implants were inserted into chest cavities of rabbit models of pectus excavatum according to Nuss procedure. The orthopedic effect were obtained by comparison of chest CT images of each rabbit model of pectus excavatum before and after operation. The deformity if full and precisely corrected from image of CT plain scan and Three Dimension Reconstruction (As shown in the **Figure 5**).

Disclosure of conflict of interest

None.

Authors' contribution

JZ and ZG conceived and designed the study, reviewed the literature, extracted data, performed statistical analyses, and drafted the manuscript. BX, CS, WY, BZ, HZ, YL, and HL were involved in critically assessing and revising the intellectual content of the manuscript. All authors read and approved the final manuscript.

Address correspondence to: Dr. Zhenguang Chen, Departments of Thoracic Surgery, Cardiothoracic Surgery of East Division, The First Affiliated Hospital, Sun Yat-sen University, 58 Zhongshan Road II, Guangzhou 510080, Guangdong, China. Tel: 86-20-87755766 Ext. 8782; Fax: 86-20-87755766 Ext. 8728; E-mail: chenzhenguang@yahoo.com

References

[1] Kim KH, Lee KY, Lee JB, Yang KS, Hwang J, Je BK, Park HJ. Radiologic factors related to double-bar insertion in minimal invasive repair of pectus excavatum. World J Pediatr 2015; 11: 148-53.

[2] Ma IT, Rebecca AM, Notrica DM, McMahon LE, Jaroszewski DE. Pectus excavatum in adult women: repair and the impact of prior or concurrent breast augmentation. Plast Reconstr Surg 2015; 135: 303e-12e.

[3] Fokin AA, Steuerwald NM, Ahrens WA, Allen KE. Anatomical, histologic, and genetic characteristics of congenital chest wall deformities. Semin Thorac Cardiovasc Surg 2009; 21: 44-57.

[4] Kelly RE, Shamberger RC. Congenital chest wall deformities. 2012; 779-808.

[5] Kotzot D, Schwabegger AH. Etiology of chest wall deformities-a genetic review for the treating physician. J Pediatr Surg 2009; 44: 2004-11.

[6] Fonkalsrud EW. Current management of pectus excavatum. World J Surg 2003; 27: 502-8.

[7] Jeong JY, Ahn JH, Kim SY, Chun YH, Han K, Sim SB, Jo KH. Pulmonary function before and after the Nuss procedure in adolescents with pectus excavatum: correlation with morphological subtypes. J Cardiothorac Surg 2015; 10: 37.

[8] Kelly RE Jr. Pectus excavatum: historical background, clinical picture, preoperative evaluation and criteria for operation. Semin Pediatr Surg 2008; 17: 181-93.

[9] Krille S, Müller A, Steinmann C, Reingruber B, Weber P, Martin A. Self- and social perception of physical appearance in chest wall deformity. Body Image 2012; 9: 246-52.

[10] Steinmann C, Krille S, Mueller A, Weber P, Reingruber B, Martin A. Pectus excavatum and pectus carinatum patients suffer from lower quality of life and impaired body image: a control group comparison of psychological characteristics prior to surgical correction. Eur J Cardiothorac Surg 2011; 40: 1138-45.

[11] Kelly RE Jr, Cash TF, Shamberger RC, Mitchell KK, Mellins RB, Lawson ML, Oldham K, Azizkhan RG, Hebra AV, Nuss D, Goretsky MJ, Sharp RJ, Holcomb GW 3rd, Shim WK, Megison SM, Moss RL, Fecteau AH, Colombani PM, Bagley T, Quinn A, Moskowitz AB. Surgical repair of pectus excavatum markedly improves body image and perceived ability for physical activity: multicenter study. Pediatrics 2008; 122: 1218-22.

[12] Kelly RE Jr, Lawson ML, Paidas CN, Hruban RH. Pectus excavatum in a 112-year autopsy series: anatomic findings and the effect on survival. J Pediatr Surg 2005; 40: 1275-8.

[13] Zhang DK, Tang JM, Ben XS, Xie L, Zhou HY, Ye X, Zhou ZH, Shi RQ, Xiao P, Chen G. Surgical correction of 639 pectus excavatum cases via the Nuss procedure. J Thorac Dis 2015; 7: 1595-605.

[14] Li G, Jiang Z, Xiao H, Wang M, Hu F, Xie X, Mei J. A novel modified Nuss procedure for pectus excavatum: a new steel bar. Ann Thorac Surg 2015; 99: 1788-92.

[15] Shamberger RC. Congenital chest wall deformities. Curr Probl Surg 1996; 33: 469-542.

[16] Wang L, Zhong H, Zhang FX, Mei J, Li GQ, Xiao HB. Minimally invasive Nuss technique allows for repair of recurrent pectus excavatum following the Ravitch procedure: report of 12 cases. Surg Today 2011; 41: 1156-60.
[17] Karner CM, Long F, Solnica-Krezel L, Monk KR, Gray RS. Gpr126/Adgrg6 deletion in cartilage models idiopathic scoliosis and pectus excavatum in mice. Hum Mol Genet 2015; 24: 4365-73.
[18] Chang PY, Zeng Q, Wong KS, Wang CJ, Chang CJ. Chest wall constriction after the nuss procedure identified from chest radiograph and multislice computed tomography shortly after removal of the bar. Thorac Cardiovasc Surg 2016; 64: 70-7.
[19] Zhao Q, Safdar N, Duan C, Sandler A, Linguraru MG. Chest modeling and personalized surgical planning for pectus excavatum. Med Image Comput Comput Assist Interv 2014; 17: 512-9.
[20] Kim HC, Choi H, Jin SO, Lee JJ, Nam KW, Kim IY, Nam KC, Park HJ, Lee KH, Kim MG. New computerized indices for quantitative evaluation of depression and asymmetry in patients with chest wall deformities. Artif Organs 2013; 37: 712-8.
[21] Glinkowski W, Sitnik R, Witkowski M, Kocoń H, Bolewicki P, Górecki A. Method of pectus excavatum measurement based on structured light technique. J Biomed Opt 2009; 14: 044041.
[22] Rodrigues PL, Rodrigues NF, Pinho AC, Fonseca JC, Correia-Pinto J, Vilaça JL. Automatic modeling of pectus excavatum corrective prosthesis using artificial neural networks. Med Eng Phys 2014; 36: 1338-45.
[23] Zhang GW, Gu TX, Guan XY, Sun XJ, Qi X, Li XY, Wang XB, Yu L, Jiang DQ, Tang R, Li-Ling J. bFGF binding cardiac extracellular matrix promotes the repair potential of bone marrow mesenchymal stem cells in a rabbit model for acute myocardial infarction. Biomed Mater 2015; 10: 065018.
[24] Olson JC, Takahashi A, Glotzbecker MP, Snyder BD. Extent of spine deformity predicts lung growth and function in rabbit model of early onset scoliosis. PLoS One 2015; 10: e0136941.
[25] Kajzer A, Kajzer W, Gzik-Zroska B, Wolański W, Janicka I, Dzielicki J. Experimental biomechanical assessment of plate stabilizers for treatment of pectus excavatum. Acta Bioeng Biomech 2013; 15: 113-21.